DALTON
FULL PAPER

A study of the asymmetry of ligands in bis(trichlorosilyl)*tert*-butylphosphine, $PBu^t(SiCl_3)_2$: molecular structure by gas-phase electron diffraction and *ab initio* calculations †

Sarah L. Hinchley,[a] Heather E. Robertson,[a] David W. H. Rankin[a] and Wolf-W. du Mont[b]

[a] *School of Chemistry, University of Edinburgh, West Mains Road, Edinburgh, UK EH9 3JJ*
[b] *Institut für Anorganische und Analytische Chemie der Technische Universität Braunschweig, Hagenring 30, D-38106 Braunschweig, Germany*

Received 17th May 2002, Accepted 6th August 2002
First published as an Advance Article on the web 13th September 2002

The molecular structure of bis(trichlorosilyl)*tert*-butylphosphine has been determined in the gas phase by electron diffraction (GED) and high level *ab initio* molecular-orbital calculations. The C_1 global minimum on the potential energy surface could be reached by twisting all three groups in the same sense by 15–20° from the fully staggered C_s conformation, found to be a saddle point and 26.7 kJ mol^{-1} higher in energy at HF/6-31G*. Important structural parameters (r_a) are: (distances) P–C 190.6(6), P–Si (mean) 221.0(5), C–C (mean) 156.5(6) and Si–Cl (mean) 203.2(1) pm; (bond angles) P–C–C (mean) 109.7(6), C–P–Si 105.0(7) and 104.5(7), Si–P–Si 99.9(6), and P–Si–Cl (mean) 111.2°; (dihedral angles) Si(7)–P–C–C 87.0(17), Si(8)–P–C–C 168.3(17), Cl(17)–Si–P–C 68.3(17) and Cl(18)–Si–P–C 80.0(10)°. Theoretical predictions at the MP2(fc)/6-31G* level were used to restrain some of the refining parameters using the SARACEN method. The angles at silicon and carbon (*tert*-butyl) were found to vary from 105.9(7) to 117.4(5)°, indicating that the three groups are greatly distorted from regular tetrahedral geometry. The axial and equatorial components of the tilts of these groups have been investigated and the *tert*-butyl group was found to tilt in the direction of the phosphorus lone pair with virtually no equatorial tilt. One $SiCl_3$ group is tilted towards the *tert*-butyl group and one tilted away, both with axial and equatorial components. The structures of the related molecules $PBu^t(SiH_3)_2$ and $PBu^t(SiH_3)(SiCl_3)$ have also been investigated by *ab initio* calculations and the distortions analysed in a similar manner to those of $PBu^t(SiCl_3)_2$.

Introduction

Phosphines normally demonstrate steeply pyramidal coordination at phosphorus. For example, angles of 96.5(5) and 95.39(5)° are observed in $P(SiH_3)_3$[1] and $P(GeH_3)_3$[2] respectively. By widening the angles at the phosphorus atom it should be possible to accommodate more bulky ligands such as $SiMe_3$ and *tert*-butyl groups. This is demonstrated in the studies of $P(SiMe_3)_3$,[3] and $PClBu^t_2$,[4] with the Si–P–Si and C–P–C angles found to be 105.1(2) and 108.9(13)° respectively. A study of PBu^t_3[5] returned C–P–C angles of 109.9(1)° and the authors noted that "the steric interactions between two *tert*-butyl groups were very similar to the steric interactions between a *tert*-butyl group and the lone electron pair".[5] In PBu^t_3O and PBu^t_3NH, the C–P–C angles were observed to be 112.9(5) and 109.4(7)°,[6] indicating that replacement of the lone pair on the phosphorus by a bonded group allows even more flexibility around the phosphorus.

The structure of $PBu^t_2(SiCl_3)$ has recently been elucidated.[7] The C–P–C angle in this case was found to be 110.6(13)°. However, the C–P–Si angles were found to be much smaller [103.4(8) and 102.8(6)°]. This can be attributed to the steric effects of the bulky *tert*-butyl groups repelling each other towards the $SiCl_3$ group, and also the electron-withdrawing effect of the $SiCl_3$ group itself. Examination of the observed tilt parameters in this molecule reveal that all the groups are tilted in an axial sense, ~6° towards the lone pair on the phosphorus. There are also small components of the tilts of these groups in the equatorial belt of the molecule. Rather surprisingly, the *tert*-butyl groups are actually tilted towards each other by ~2°, an indication that any residual interactions between the two groups after widening of the C–P–C angle are less than those between the *tert*-butyl groups and the $SiCl_3$ group.[7]

These groups of molecules are interesting from the point of view of steric interactions between the groups themselves and with the lone pair of electrons present on the phosphorus atom. Having studied $PBu^t_2(SiCl_3)$ and determined the behaviour of the groups, it was decided to study the related molecule $PBu^t(SiCl_3)_2$. The presence of two electron-withdrawing groups and the lone pair is likely to give rise to some interesting behaviour of the ligands, both in the bond lengths and angles, and in the twists and tilts of the groups in relation to each other and the lone pair. In conjunction with this work, the structures of $PBu^t(SiH_3)_2$ and $PBu^t(SiCl_3)(SiH_3)$ were also studied by *ab initio* calculations to evaluate the magnitude and directions of the tilts in these related compounds.

Experimental

Synthesis

A sample of $PBu^t(SiCl_3)_2$ was prepared by the literature method.[8]

Theoretical methods

All calculations were performed on a Dec Alpha 1000 4/200 workstation using the Gaussian 98 program.[9] An extensive search of the torsional potentials of $PBu^t(SiCl_3)_2$, $PBu^t(SiH_3)_2$ and $PBu^t(SiCl_3)(SiH_3)$ was undertaken at the HF/3-21G* [10–12] level in order to locate all minima. For $PBu^t(SiCl_3)_2$ and PBu^t-

† Electronic supplementary information (ESI) available: tables of theoretical and calculated geometrical parameters; experimental coordinates for $PBu^t(SiCl_3)_2$ from the GED analysis. See http://www.rsc.org/suppdata/dt/b2/b204823j/

DOI: 10.1039/b204823j

$(SiH_3)_2$, one conformer of C_1 symmetry was located and further geometry optimisations were undertaken at the HF and MP2(fc) levels using the standard 6-31G* [13–15] basis set, and at the MP2(fc)/6-311G* level.[16] For $PBu^t(SiCl_3)(SiH_3)$, two C_1 conformers were located, differing primarily in the direction of twist of the three ligands. Further calculations were performed on each in a similar manner to the previous molecules. Calculations were also performed to analyse the charge distribution in the molecules. As atomic charge is not a quantum mechanical observable, the four main methods to partition the electron density among the atoms in the molecular systems were explored.[17] These were the Mulliken population analysis, Natural Population Analysis,[17a] and the electrostatic potential-derived charges using the CHelpG scheme of Breneman,[17b] and that of Merz–Kollman–Singh (MK).[17c]

Analytic second derivatives of the energy with respect to nuclear coordinates calculated at the HF/3-21G* and HF/6-31G* levels for $PBu^t(SiCl_3)_2$ gave the force field, which was used to provide estimates of the amplitudes of vibration (u) for use in the gas electron diffraction (GED) refinements. The force fields for all the calculated structures were also used to calculate the frequencies, which in turn provided information about the nature of stationary points and were compared with experimentally determined frequencies where these were available. Calculating the force fields at the MP2(fc) level of theory would make little difference to the vibrational quantities and for this size of molecule was deemed unnecessary. The structure of $PBu^t(SiCl_3)_2$ with the atom numbering scheme is shown in Fig. 1.

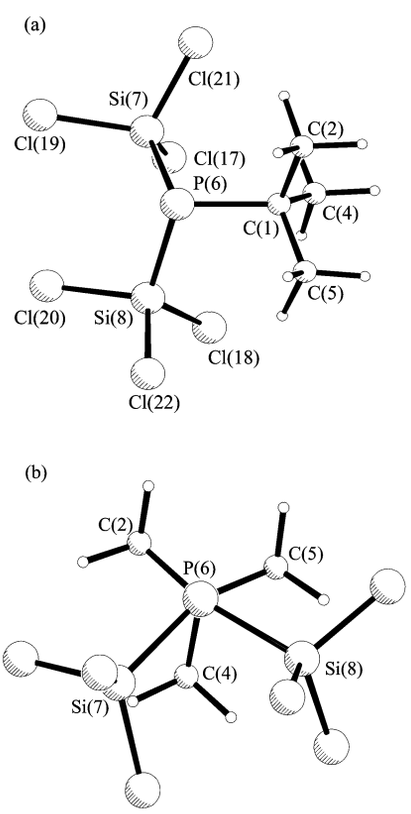

Fig. 1 Molecular structure of $PBu^t(SiCl_3)_2$ in the gas phase. (a) Perspective view. (b) View along the P–C bond.

Gas-phase electron diffraction

Data were collected for $PBu^t(SiCl_3)_2$ using the Edinburgh gas diffraction apparatus.[18] An accelerating voltage of *ca.* 40 kV (electron wavelength *ca.* 6.0 pm) was used, whilst maintaining the sample and nozzle temperatures at 408 and 435 K. Scattering intensities were recorded at nozzle-to-plate distances of 90 and 257 mm on Kodak Electron Image plates. Four plates were collected at the short distance and five at the long distance. The weighting points for the off-diagonal weight matrices, correlation parameters and scale factors for the two camera distances are given in Table 1, together with electron wavelengths. These were determined from the scattering patterns of benzene vapour, recorded immediately after the patterns of $PBu^t(SiCl_3)_2$ and analysed in exactly the same way, to minimise systematic errors in wavelengths and camera distances. The electron-scattering patterns were converted into digital form using a PDS densitometer at the Institute of Astronomy in Cambridge with a scanning program described elsewhere.[19] Data reduction and least-squares refinements were carried out using standard programs,[20,21] employing the scattering factors of Ross *et al.*[22]

Table 1 Nozzle-to-plate distances (mm), weighting functions (nm^{-1}), correlation parameters, scale factors and electron wavelengths (pm) used in the electron-diffraction study

Nozzle-to-plate distance[a]	89.56	256.76
Δs	4	2
s_{min}	84	26
sw_1	104	46
sw_2	260	130
s_{max}	340	152
Correlation parameter	0.2702	0.4781
Scale factor[b]	0.523(14)	0.808(8)
Electron wavelength	6.016	6.016

[a] Determined by reference to the scattering pattern of benzene vapour. [b] Values in parentheses are the estimated standard deviations.

Results

Ab initio calculations

A series of molecular orbital calculations was undertaken to investigate the structures of $PBu^t(SiCl_3)_2$, $PBu^t(SiH_3)_2$ and $PBu^t(SiCl_3)(SiH_3)$. Preliminary investigations of $PBu^t(SiCl_3)_2$ assuming all the groups to be fully staggered, with overall C_s symmetry, returned two imaginary frequencies (256i and 30i cm^{-1}) at the HF/6-31G* level, indicating that the C_s structure is a saddle point on the potential energy surface. Further investigation of the structure in C_1 symmetry revealed that the minimum could be reached by twisting the *tert*-butyl and trichlorosilyl groups in the same sense by 15–20° from the staggered (C_s) conformation. This resulted in a reduction of the molecular energy of the system by 26.7 kJ mol^{-1} at the HF/6-31G* level. The C_s conformation is a saddle point on the potential energy surface and the transition between the two minima must not simply involve concerted rotation of the three groups. Similar minima were observed for $PBu^t(SiH_3)_2$. In the case of $PBu^t(SiCl_3)(SiH_3)$, two local minima were observed, each having C_1 symmetry. One conformer can be thought of as having all three bulky ligands twisted by 15–20° from the perfectly staggered form in the same sense, and the other conformer has all three ligands twisted by 15–20° in the opposite sense.

Further calculations for all molecules at the MP2(fc)/6-31G* and MP2(fc)/6-311G* levels were performed in C_1 symmetry. The molecular geometries for all four molecules at the MP2(fc)/6-311G* level are presented in Table 2, and at the MP2(fc)6-31G* level for $PBu^t(SiCl_3)_2$ in Table 3. Those calculated at the HF/6-31G* level of theory for all the C_1 structures and the C_s structure of $PBu^t(SiCl_3)_2$ and at the MP2(fc)6-31G* level for $PBu^t(SiH_3)_2$ and the two conformers of $PBu^t(SiCl_3)(SiH_3)$ are given as ESI (Tables S1 and S2). As the molecules do not contain any significant double-bond character but have electronegative atoms and lone pairs, including the effects of electron correlation with the further level of theory and larger basis set is important. Generally the bond lengths and angles did not change more than 1 pm or 1° upon going from HF/6-31G* to

Table 2 Calculated geometric parameters (r_a structure) for $PBu^t(SiCl_3)_2$, $PBu^t(SiH_3)_2$ and the two conformers of $PBu^t(SiH_3)(SiCl_3)$ (distances in pm, angles in °) at the MP2(fc)/6-311G* level

Geometrical parameter	$PBu^t(SiCl_3)_2$	$PBu^t(SiH_3)_2$	$PBu^t(SiH_3)(SiCl_3)$[a] (A)	$PBu^t(SiH_3)(SiCl_3)$[a] (B)
P–C	190.0	189.6	189.7	189.7
C–C (mean)	153.3	153.2	153.3	153.3
P–Si(7)	223.8	225.0	226.3	226.3
P–Si(8)	223.7	224.8	221.8	221.6
C–H (mean)	109.3	109.5	109.4	109.4
Si–H (mean)	—	148.3	148.0	148.0
Si–Cl (mean)	203.8	—	204.6	204.6
P–C(1)–C(2)	105.4	106.4	106.1	104.7
P–C(1)–C(4)	115.4	114.9	115.4	115.0
P–C(1)–C(5)	107.3	107.4	106.7	108.6
C–C–C (mean)	109.5	109.3	109.5	109.4
H–C–H (mean)	108.0	107.9	108.0	107.6
C–P–Si(7)	107.0	104.5	104.6	104.8
C–P–Si(8)	106.3	104.2	106.5	106.6
Si(7)–P–Si(8)	101.1	97.0	97.3	99.1
P–Si(7)–X(17)[b]	116.3	114.5	113.1	114.0
P–Si(7)–X(19)	108.3	106.7	106.8	106.9
P–Si(7)–X(21)	109.1	109.0	107.5	106.4
P–Si(8)–Y(18)[b]	117.3	114.3	117.0	117.7
P–Si(8)–Y(20)	109.0	106.2	107.4	107.4
P–Si(8)–Y(22)	107.6	109.9	111.0	110.3
C–P–Si(7)–X(17)	70.9	65.3	37.6	66.4
C–P–Si(8)–Y(18)	−38.1	−42.9	−66.1	−42.8
Absolute energy[c]	−3834.3866	−1079.6875	−2457.0398	−2457.0393

[a] A = Lower energy conformer, B = Higher energy conformer. [b] X and Y = H or Cl. [c] Energy in Hartrees.

Table 3 Refined and calculated geometric parameters (r_a structure) for $PBu^t(SiCl_3)_2$ (distances in pm, angles in °) from the GED study[a]

No.	Parameter	GED (r_a)	MP2(fc)/6-31G*	Restraint
Independent parameters				
p_1	C–H	112.9(15)	109.5	109.0(30)
p_2	P–C	190.6(6)	190.8	190.1(10)
p_3	C–C	156.5(6)	153.2	154.0(10)
p_4	P–Si	221.0(5)	224.0	—
p_5	Si–Cl	203.2(1)	204.4	—
p_6	C–C–H	111.8(5)	112.0	111.9(5)
p_7	P–C–C mean	109.7(6)	109.3	—
p_8	[P–C–C(2)] − [P–C–C(4)]	−9.2(9)	−9.5	−9.5(10)
p_9	[P–C–C(2)] − [P–C–C(5)]	−2.1(10)	−1.7	−1.8(10)
p_{10}	P–Si–Cl mean	111.1(2)	111.2	111.2(5)
p_{11}	[P–Si–Cl av. (gp1)] − [P–Si–Cl av. (gp2)]	−0.04(2)	−0.04	−0.04(2)
p_{12}	[P–Si(7)–Cl(17)] − [P–Si(7)–Cl(19)]	8.8(10)	8.6	8.6(10)
p_{13}	[P–Si(7)–Cl(17)] − [P–Si(7)–Cl(21)]	6.9(9)	7.5	7.5(10)
p_{14}	[P–Si(8)–Cl(18)] − [P–Si(8)–Cl(20)]	8.1(9)	8.7	8.7(10)
p_{15}	[P–Si(8)–Cl(18)] − [P–Si(8)–Cl(22)]	10.6(9)	9.8	9.8(10)
p_{16}	C–P–Si mean	104.7(7)	107.4	—
p_{17}	[C–P–Si(7)] − [C–P–Si(8)]/2	0.5(2)	0.5	0.5(2)
p_{18}	$SiCl_3$ dihedral av. {ϕ[C(2)–C(1)–P(6)–Si(7)] + ϕ[C(2)–C(1)–P(6)–Si(8)]}/2	127.6(4)	125.8	—
p_{19}	$SiCl_3$ dihedral diff. {ϕ[C(2)–C(1)–P(6)–Si(7)] − ϕ[C(2)–C(1)–P(6)–Si(8)]}/2	40.6(17)	38.6	38.6(20)
p_{20}	Methyl torsion	−63.6(20)	−64.2	−64.2(20)
p_{21}	{ϕ[C(2)–C(1)–P(6)–C(4)] + ϕ[C(2)–C(1)–P(6)–C(5)]} / 2	118.4(10)	118.4	118.4(10)
p_{22}	ϕ[C(2)–C(1)–P(6)–C(4)]–ϕ[C(2)–C(1)–P(6)–C(5)]	2.9(10)	2.8	2.8(10)
p_{23}	{ϕ[Cl(17)–Si(7)–P(6)–Cl(19)] + ϕ[Cl(17)–Si(7)–P(6)–Cl(21)]}/2	122.3(10)	122.0	122.0(10)
p_{24}	ϕ[Cl(17)–Si(7)–P(6)–Cl(19)] − ϕ[Cl(17)–Si(7)–P(6)–Cl(21)]	0.04(5)	0.1	0.1(5)
p_{25}	{ϕ[Cl(18)–Si(8)–P(6)–Cl(20)] + ϕ[Cl(18)–Si(8)–P(6)–Cl(22)]}/2	121.4(10)	121.7	121.7(10)
p_{26}	ϕ[Cl(18)–Si(8)–P(6)–Cl(20)] − ϕ[Cl(18)–Si(8)–P(6)–Cl(22)]	1.0(1)	1.0	1.0(1)
p_{27}	$SiCl_3$ ϕ av. {ϕ[Cl(17)–Si(7)–P(6)–C(1)] + ϕ[Cl(18)–Si(8)–P(6)–C(1)]}/2	52.9(12)	55.4	—
p_{28}	$SiCl_3$ ϕ diff. {ϕ[Cl(17)–Si(7)–P(6)–C(1)] − ϕ[Cl(18)–Si(8)–P(6)–C(1)]}/2	15.4(10)	17.5	—
Dependent parameters				
p_{29}	Si–P–Si	99.9(6)	101.5	—
	Absolute energy[b]		−3834.0656	

[a] Figures in parentheses are the estimated standard deviations of the last digits. See text for parameter definitions. [b] Energy in Hartrees.

the MP2(fc)/6-31G* level of theory, or from the 6-31G* to the 6-311G* basis set. For example, the P–C bond lengths are predicted to shorten on average by 0.7 pm from the HF level to the MP2(fc) level. The P–Si bond lengths changed only by ~1.1 pm for those associated with the silyl groups from the HF to the MP2(fc) level. However, those associated with the trichlorosilyl groups were observed to shorten by an average of 1.8 pm. This indicates that the inclusion of electron correlation at the MP2(fc) level is especially important in these cases with the adjacent electronegative atoms. The same bond lengths were

observed to change very little upon increasing the basis set size to 6-311G*. The C–P–Si(7/8) angles were observed to change appreciably from the HF to the MP2(fc) level. For example, in $PBu^t(SiCl_3)_2$ they changed from 109.5 and 108.7° at the HF level to 107.9 and 106.9° at the MP2(fc) level, while in $PBu^t(SiH_3)_2$, they decreased from 106.8 and 107.0° to 104.6 and 104.8°, a change of 2.2°. The use of the larger basis set also led to changes of up to 0.9°, for example in $PBu^t(SiCl_3)_2$ the C–P–Si angles were calculated to be 107.0 and 106.3° compared to 107.9 and 106.9° at the MP2(fc)/6-31G* level. The Si–P–Si angles were also observed to change significantly from the HF to the MP2(fc) level in all cases, with a change from 104.2 to 101.5° for $PBu^t(SiCl_3)_2$, and 102.3 to 99.7° for the A form of $PBu^t(SiH_3)(SiCl_3)$. However, very little change was observed to the P–Si–X/Y angles. For example, the predicted P–Si(7)–Cl(17) angle in $PBu^t(SiCl_3)_2$ hardly changed from the HF (116.4°) to the MP2(fc) (116.5°) level. The equivalent P–Si(7)–H(17) angle in the right-handed form of $PBu^t(SiH_3)(SiCl_3)$ also only changed by 0.1° from the HF to the MP2(fc) level (113.3 to 113.4°), indicating that this was not just restricted to the trichlorosilyl groups. On increasing the basis set from 6-31G* to 6-311G*, the Si–P–Si angle decreased from 98.4 to 97.0° for $PBu^t(SiH_3)_2$, while only small decreases of ~0.5° were observed for $PBu^t(SiCl_3)_2$ and the two conformers of $PBu^t(SiH_3)(SiCl_3)$. The P–Si–X/Y angles varied by ~0.5°.

Gas electron diffraction study

On the basis of the *ab initio* calculations described above, electron-diffraction refinements were carried out using a model of C_1 symmetry to describe the molecular structure. The large number of geometric parameters needed to define the model made it necessary to make the assumption of local C_{3v} symmetry for the C-methyl groups.

The structure of $PBu^t(SiCl_3)_2$ was finally defined in terms of twenty-eight independent geometric parameters, comprising five bond lengths, twelve bond angles and eleven torsion parameters (Table 3; atom numbering shown in Fig. 1).

On the basis of the highest level *ab initio* calculations, all bond lengths of the same type were assumed to be equal, with any small differences fixed at zero. The independent distance parameters are then the C–H, P–C, C–C, P–Si and Si–Cl distances (p_1–p_5). All C–C–H bond angles (p_6) were assumed to be identical. The P–C–C angles were defined in terms of the average (p_7) of P(6)–C(1)–C(2), P(6)–C(1)–C(4) and P(6)–C(1)–C(5), and two difference parameters, which were included in the refinement procedure since the butyl group was predicted to have C_1 local symmetry. The differences were described as P(6)–C(1)–C(2) minus P(6)–C(1)–C(4) (p_8) and P(6)–C(1)–C(2) minus P(6)–C(1)–C(5) (p_9).

The trichlorosilyl groups were also calculated to have C_1 local symmetry, and the P–Si–Cl angles were defined in terms of an average (p_{10}) of all the P–Si–Cl angles, and five difference parameters. The first of these differences is the average P–Si–Cl bond angle for the first $SiCl_3$ group minus the average P–Si–Cl bond angle for the second group (p_{11}). The remaining four are internal differences within the individual $SiCl_3$ groups *i.e.* P(6)–Si(7)–Cl(17) minus P(6)–Si(7)–Cl(19) (p_{12}), P(6)–Si(7)–Cl(17) minus P(6)–Si(7)–Cl(21) (p_{13}), P(6)–Si(8)–Cl(18) minus P(6)–Si(8)–Cl(20) (p_{14}) and P(6)–Si(8)–Cl(18) minus P(6)–Si(8)–Cl(22) (p_{15}).

There are three angles to be defined at the central phosphorus atom. An average (p_{16}) and a difference (p_{17}) C–P–Si angle were introduced, as were two dihedral angles (p_{18} and p_{19}) relating the central Si atoms of each $SiCl_3$ group to C(2) of the *tert*-butyl group. These two parameters define the Si–P–Si angle and the torsion angle of the butyl group *i.e.* around the C–P bond axis.

The remaining eleven parameters represent the torsion angles of the methyl, butyl and trichlorosilyl groups. The methyl groups were generated initially by placing a methyl group carbon atom at the origin, with its three H atoms arranged with local C_{3v} symmetry about the x axis and one H in the xy plane in the positive x and y directions. The methyl torsion parameter (p_{20}) is a rotation about the local x axis. The methyl group is then translated along the positive x axis by the C–C bond length and the central carbon of the *tert*-butyl group is placed at the origin. The correct C–C–C bond angles are generated by rotating the methyl group about the z axis, moving the methyl carbon atom in the positive y direction, and then generating the other methyl groups by rotation of the first group about the local x axis by two different torsion angles (p_{21} and $-p_{22}$). The *tert*-butyl group is then translated along the positive x axis by the P–C bond length.

The $SiCl_3$ groups are generated in a similar way to the methyl groups in the negative x axis direction. The first chlorine is placed in the xy plane, in the negative x and positive y directions. The remaining two chlorine atoms of each group are placed adjacent to the initial chlorine, each with its correct P–Si–Cl angle, and then rotated about the z axis by the correct torsion angles (p_{23}–p_{26}) to generate the two $SiCl_3$ groups. The $SiCl_3$ torsion angle parameters (p_{27} and p_{28}) are rotations of the groups about the local x axis.

The starting parameters for the r_a refinement were taken from the theoretical geometry optimised at the MP2(fc)/6-31G* level. The r_α structure was not refined because the rectilinear vibrational corrections (*i.e.* parallel and perpendicular correction terms) are known to be unreliable for a molecule of this size with many low-lying vibrational modes. Theoretical (HF/6-31G*) Cartesian force fields were obtained and converted into force fields described by a set of symmetry coordinates using a version of the ASYM 40 program[23] modified to work for molecules with more than 40 atoms. All geometric parameters were then refined.

In total twenty-eight geometric parameters and fourteen groups of vibrational amplitudes were refined. Flexible restraints, twenty-one geometric and five of amplitudes, were employed during the refinement using the SARACEN method.[24] These are listed in Tables 3 and 5.

The success of the final refinement, for which $R_G = 0.080$ ($R_D = 0.048$), can be assessed on the basis of the radial distribution curve (Fig. 2) and the molecular scattering intensity curves (Fig. 3). Final refined parameters are listed in Table 3, the least-squares correlation matrix is shown in Table 4, and interatomic distances and the corresponding amplitudes of vibration in Table 5. Table 6 lists all the final experimental bond angles at the butyl carbon and the silicon atoms. Experimental coordinates from the GED analysis are given in the ESI (Table S3). In the SARACEN analysis, because all parameters are refining, the error estimates are realistic. We therefore quote the estimated standard deviations, σ, and do not need to add any further allowance for fixed parameters. Fig. 1 shows a

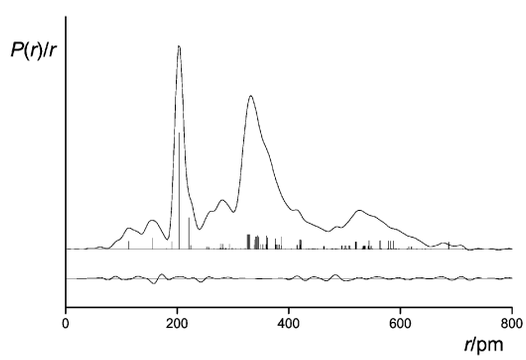

Fig. 2 Experimental and difference (experimental − theoretical) radial-distribution curves, $P(r)/r$, for $PBu^t(SiCl_3)_2$. Before Fourier inversion the data were multiplied by $s\cdot\exp(-0.00002s^2)/(Z_{Cl} - f_{Cl})/(Z_C - f_C)$.

Table 4 Least-squares correlation matrix (×100) for $PBu^t(SiCl_3)_2$ [a]

	p_3	p_4	p_{10}	p_{12}	p_{28}	u_1	u_9
p_7	−51						
p_{10}					72		
p_{20}		64	−56		−58		
u_{12}				−71			
u_{17}							−57
k_2						72	

[a] Only elements with absolute values ≥50% are shown; k_2 is a scale factor.

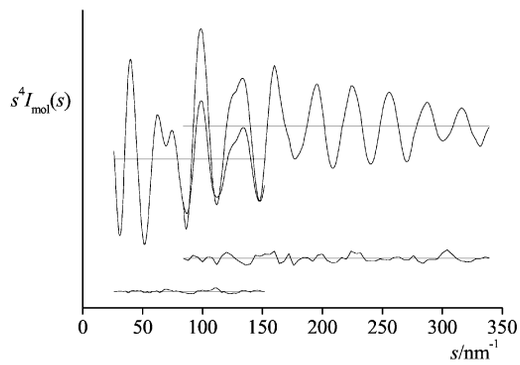

Fig. 3 Experimental and final weighted difference (experimental − theoretical) molecular-scattering intensities for $PBu^t(SiCl_3)_2$.

perspective view of $PBu^t(SiCl_3)_2$ in the optimum refinement of the GED data as well as the view down the P–C bond.

Discussion

The structural properties of $PBu^t(SiCl_3)_2$ have been investigated in the gas phase by gas-phase electron diffraction and theoretical calculations. The perfectly staggered C_s structure was found to be a saddle point on the potential energy surface of $PBu^t(SiCl_3)_2$, with the C_1 structure where all the groups are twisted by 15–20° found to be the preferred structure. Torsion angles in this range are the norm for moieties of the general type $A(BC_3)_3$, because this minimises 1,3-C···C interactions. For example, the $PBu^t_2(SiCl_3)$ analogue also exhibits this behaviour,[7] with both the *tert*-butyl groups and the $SiCl_3$ group twisted by about 17° from the perfectly staggered positions, and each of the three groups tilted about 6° away from each other (towards the phosphorus lone pair) to reduce steric strain. Tri-*tert*-butylphosphine oxide[25] exhibits a twist of the butyl groups by 15.8(7)° with tilts of 3.1(8)°, and the related tri-*tert*-butylphosphine imide[25] shows twists of 18.5(14)°, but interestingly shows tilts of −2.3(11)°, indicating that the groups all tilt away from the NH group. In the last two examples, the O and the NH groups are protected from attack by the orientation of the bulky ligands, and this provides an explanation for the thermodynamic and chemical stability of these compounds.

Overall, there is reasonable agreement between the experimental and theoretical structures. Theoretical bond lengths were generally found to be within 1–2 pm of the experimental values, the exceptions being the C–H and P–Si bond lengths. The P–Si bond lengths were calculated to be 223.8 and 223.7 pm, compared to the experimental value of 221.0 pm. The experimental value is an r_a distance and the r_e distance, equivalent to the computed parameter, would be almost exactly the same. The computed [MP2(fc)/6-311G*] distance at this level is clearly overestimated for this parameter, as are the MP2(fc)/6-31G* values (224.0 pm). This is typical for 2nd row atoms, with the MP2(fc)/6-31G* method giving errors in bond lengths between first and second row atoms.[26] In tetramethylsilane,[27] the Si–C bond lengths were overestimated by about 2 pm at this level, whilst in cyclobutyltrifluorosilane,[28] the Si–F distance was calculated to be 2.3 pm too long compared to the GED results. Theoretical bond angles also tended to be within 1–2° of those found experimentally, although the angles around the phosphorus atom were overestimated. For example, the C–P–Si(7/8) angles were predicted to be 107.0 and 106.3° as compared to 105.0 and 104.5° found experimentally. Similarly, the Si–P–Si angle was also overestimated theoretically, 101.1 compared to 99.9° found experimentally.

The related structures of $PBu^t(SiH_3)_2$ and $PBu^t(SiH_3)(SiCl_3)$ have also been investigated by *ab initio* calculations. $PBu^t(SiH_3)_2$ was found to adopt a similar structure to $PBu^t(SiCl_3)_2$, with all three bulky groups twisted in the same sense by ~15°. The P–SiH_3 bonds were found to be slightly longer than the equivalent P–$SiCl_3$ bonds in $PBu^t(SiCl_3)_2$ (225.0 and 224.8 pm compared to 223.8 and 223.7 pm) at the MP2(fc)/6-311G* level. This can be attributed to the electron density in the P–Si bond being pulled

Table 5 Interatomic distances (r_a/pm) and amplitudes of vibration (u/pm) for the restrained GED structure of $PBu^t(SiCl_3)_2$ [a]

No.	Atom pair	r_a/pm	u/pm [b]	Restraint
u_1	Cl(17)–Si(7)	203.2(1)	3.8(2)	—
u_2	Si(7)–P(6)	221.0(5)	6.2(5)	—
u_3	Cl(20)···Cl(18)	327.3(20)	9.5(4)	—
u_4	Cl(21)···Cl(19)	325.8(36)	9.3(tied to u_3)	—
u_5	Cl(21)···Cl(17)	328.1(21)	9.5(tied to u_3)	—
u_6	Cl(22)···Cl(18)	327.2(19)	9.5(tied to u_3)	—
u_7	Cl(22)···Cl(20)	330.0(36)	9.4(tied to u_3)	—
u_8	Cl(19)···Cl(17)	330.5(21)	9.5(tied to u_3)	—
u_9	Cl(20)···Cl(19)	344.4(14)	5.2(15)	—
u_{10}	Cl(18)···Cl(17)	360.3(24)	7.2(tied to u_9)	—
u_{11}	Cl(20)···Cl(17)	387.1(75)	41.0(fixed)	—
u_{12}	Cl(20)···P(6)	340.7(15)	21.4(38)	—
u_{13}	Cl(19)···P(6)	342.4(18)	21.2(tied to u_{12})	—
u_{14}	Cl(22)···P(6)	346.1(14)	20.6(tied to u_{12})	—
u_{15}	Cl(21)···P(6)	346.4(15)	20.9(tied to u_{12})	—
u_{16}	C(2)–C(1)	156.5(6)	5.9(5)	5.1(5)
u_{17}	Cl(17)···P(6)	360.5(11)	13.2(22)	—
u_{18}	Cl(18)···P(6)	362.6(12)	13.1(tied to u_{17})	—
u_{19}	Cl(20)···Si(7)	362.3(34)	20.5(19)	19.9(19)
u_{20}	Cl(17)···Si(8)	376.4(28)	23.8(tied to u_{19})	—
u_{21}	Si(8)···Si(7)	338.5(13)	10.6(10)	10.5(10)
u_{22}	Cl(19)···Si(8)	420.4(16)	16.0(15)	—
u_{23}	Cl(18)···Si(7)	422.7(16)	18.7(tied to u_{22})	—
u_{24}	Cl(19)···Cl(18)	544.1(33)	25.7(26)	27.7(27)
u_{25}	Cl(21)···Cl(20)	563.9(32)	17.5(tied to u_{24})	—
u_{26}	H(3)–C(2)	112.9(14)	7.6(7)	7.4(7)
u_{27}	Cl(22)···Cl(19)	582.7(32)	23.2(17)	—
u_{28}	Cl(22)···Cl(17)	578.8(26)	22.5(tied to u_{27})	—
u_{29}	Cl(21)···Cl(18)	588.0(32)	24.2(tied to u_{27})	—
u_{30}	P(6)–C(1)	190.6(9)	9.3(tied to u_1)	—
u_{31}	Cl(21)···Si(8)	519.8(13)	13.2(14)	—
u_{32}	Cl(22)···Si(7)	521.5(14)	13.5(tied to u_{31})	—
u_{33}	Cl(22)···Cl(21)	686.7(14)	13.6(fixed)	—
u_{34}	P(6)···C(2)	277.8(13)	5.3(17)	—
u_{35}	P(6)···C(5)	281.4(13)	5.4(tied to u_{34})	—
u_{36}	P(6)···C(4)	293.4(16)	5.1(tied to u_{34})	—

[a] Estimated standard deviations, obtained in the least-squares refinement, are given in parentheses. [b] Amplitudes not refined were fixed at the values obtained using the HF/6-31G* force field.

Table 6 Angles at the central atoms of the *tert*-butyl and two $SiCl_3$ groups (angles in °) from the final GED refinement of $PBu^t(SiCl_3)_2$

P(6)–C(1)–C(2)	105.9(7)	Cl(17)–Si(7)–Cl(19)	107.3(9)
P(6)–C(1)–C(4)	115.1(9)	Cl(17)–Si(7)–Cl(21)	107.2(9)
P(6)–C(1)–C(5)	107.9(8)	Cl(19)–Si(7)–Cl(21)	108.6(17)
C(2)–C(1)–C(4)	109.7(14)	P(6)–Si(8)–Cl(18)	117.4(5)
C(2)–C(1)–C(5)	108.0(13)	P(6)–Si(8)–Cl(20)	106.8(6)
C(4)–C(1)–C(5)	109.9(17)	P(6)–Si(8)–Cl(22)	109.3(6)
P(6)–Si(7)–Cl(17)	116.3(5)	Cl(18)–Si(8)–Cl(20)	108.8(10)
P(6)–Si(7)–Cl(19)	107.5(8)	Cl(18)–Si(8)–Cl(22)	107.6(10)
P(6)–Si(7)–Cl(21)	109.4(7)	Cl(20)–Si(8)–Cl(22)	106.6(17)

towards the silicon by the electronegative chlorine atoms. This makes the phosphorus more negative, and the silicon more positive, and hence an overall shortening of the P–Si bond is observed due to the electrostatic interactions.

$PBu^t(SiH_3)(SiCl_3)$ can adopt two different conformations because the three groups bound to P are all different. Both these structures were investigated by *ab initio* calculations and were found to be minima on the potential energy surface. One has all three ligands twisted in the same sense by ~15° from the perfectly staggered form. The other conformer has all three ligands twisted by ~15° in the opposite sense. One of them was found to be the more stable by 1.3 kJ mol^{-1} at the MP2(fc)/6-311G* level. We call this conformer A, and the less stable one B. From our calculations we can infer that there would be 59% of A and 41% of B in a mixture at room temperature.

The observed P–Si bond lengths were ~224 and 225 pm for $PBu^t(SiH_3)_2$ and $PBu^t(SiCl_3)_2$ at the MP2(fc)/6-311G* level and we can conclude that the competition for electron density by the silyl groups is equally balanced in each of these molecules. In $PBu^t(SiH_3)(SiCl_3)$, we have an unbalanced case, and the P–SiH_3 bond is lengthened to ~226 pm and the P–$SiCl_3$ bond is shortened to ~222 pm in both conformers.

To confirm or deny this theory, charge density calculations were performed to determine the charges on the phosphorus and silicon atoms to see how they affect the bond lengths. Four different techniques were used so that we could compare the methods: Mulliken population analysis, Natural Population Analysis, and the electrostatic potential-derived charges using the CHelpG scheme of Breneman, and that of Merz–Kollman–Singh (MK). The results are summarised in Table 7. Initially it can be seen that similar trends are observed for the Mulliken and NPA methods, and for the MK and CHelpG methods. Results from the MK and CHelpG methods were discounted as the charges on the two Si atoms were calculated to be approximately the same, and this observation cannot explain the difference in the P–Si bond lengths observed. Of all the calculations performed, the results from the Mulliken charge density calculations are the most believable. For $PBu^t(SiCl_3)_2$ and $PBu^t(SiH_3)_2$, the results are very similar to those from the NPA analysis, with approximately neutral charge observed on the phosphorus and equal charges on the silicon atoms. However, for $PBu^t(SiCl_3)(SiH_3)$, we see a large increase of electron density on phosphorus and Si(7)(H_3) relative to both compounds with two equivalent SiX_3 groups. Si(8)(Cl_3) has a small increase in electron density relative to $PBu^t(SiCl_3)_2$, but a small decrease relative to $PBu^t(SiH_3)_2$. There is an attractive force between the negative P and the positive Si(8), and therefore a shorter P–Si(8) bond distance is calculated for $PBu^t(SiCl_3)(SiH_3)$ than $PBu^t(SiCl_3)_2$. There is a repulsive force between the negative P and the negative Si(7) which accounts for the longer P–Si(7) bond calculated for $PBu^t(SiCl_3)(SiH_3)$ than for $PBu^t(SiH_3)_2$. Although a reasonable argument can be derived from the Mulliken charge density calculations to explain the observed lengthening and shortening of the P–Si bonds, the other three types of calculation do not offer any explanation for this phenomenon.

In all the molecules the ligands are distorted; this can be studied by examining the tilt angles associated with them. In all cases, the SiX_3 groups and the *tert*-butyl group were observed to have approximate three-fold local symmetry. However, the local axes do not coincide with either the P–Si or the P–C bonds. The magnitudes of the tilts of the groups away from the bonds can be represented by one parameter for each group. For example, if we consider the Si(7)X_3 group, the centroid of the triangle created by the 3H or Cl atoms [X(17), X(19) and X(21)] can be represented by V and the angle created by V–Si and the Si–P bond is the tilt parameter. If we consider the other SiY_3 group and the *tert*-butyl group in the same manner, with W representing the centroid of the Y(18)···Y(20)···Y(22) triangle and X the centroid of the C(2)···C(4)···C(5) triangle, tilt

Table 7 Charge distributions for $PBu^t(SiCl_3)_2$, the two conformers of $PBu^t(SiCl_3)(SiH_3)$ and $PBu^t(SiH_3)_2$ at the MP2/6-311G* level

	NPA	Mulliken	MK	CHelpG
$PBu^t(SiCl_3)_2$				
C(1)	−0.27	−0.36	0.73	0.82
P(6)	−0.02	−0.01	−0.34	−0.49
Si(7)	1.05	0.95	0.34	0.65
Si(8)	1.05	0.95	0.36	0.63
$PBu^t(SiCl_3)(SiH_3)$ (A)				
C(1)	−0.27	−0.21	0.79	0.83
P(6)	0.00	−0.65	−0.53	−0.58
Si(7)	0.57	−0.17	0.69	0.72
Si(8)	1.04	0.75	0.51	0.70
$PBu^t(SiCl_3)(SiH_3)$ (B)				
C(1)	−0.27	−0.21	0.81	0.84
P(6)	0.01	−0.65	−0.53	−0.58
Si(7)	0.57	−0.17	0.68	0.74
Si(8)	1.04	0.75	0.48	0.71
$PBu^t(SiH_3)_2$				
C(1)	−0.28	−0.35	0.92	0.83
P(6)	0.02	−0.07	−0.72	−0.65
Si(7)	0.56	0.47	0.84	0.75
Si(8)	0.56	0.47	0.80	0.75

Table 8 Tilt angles for $PBu^t(SiH_3)_2$, $PBu^t(SiH_3)(SiCl_3)$ and $PBu^t(SiCl_3)_2$[a]

	X, Y = H	X = H, Y = Cl (B)	X = H, Y = Cl (A)	X, Y = Cl
Si(7)X_3	4.1	5.0	3.6	5.8
Si(8)Y_3	4.3	6.2	5.0	5.6
C(1)C_3	5.6	6.2	6.7	6.8

[a] All angles in °.

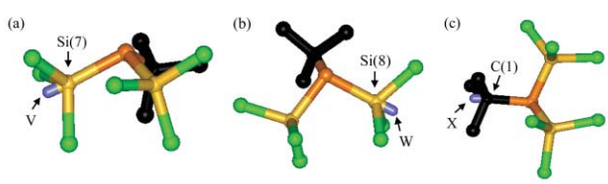

Fig. 4 Diagrammatic representation of (a) V for the Si(7)Cl_3 group, (b) W for the Si(8)Cl_3 group and (c) X for the C(1)C_3 group.

parameters for each group can be defined. Centroids V, W and X for $PBu^t(SiCl_3)_2$ are shown in Fig. 4. The tilt angles for all four molecules are given in Table 8.

The direction of the tilt of each group is determined by initially introducing a point Y along the P–C(1) vector at a distance equivalent to the P–Si distance, then defining Z as the centroid of the Y···Si(7)···Si(8) triangle. This is shown in Fig. 5 for $PBu^t(SiCl_3)_2$. The tilt direction for the *tert*-butyl group ϕ[X–C(1)–P(6)–Z], and the two SiX/Y_3 groups, ϕ[V–Si(7)–P(6)–Z] and ϕ[W–Si(8)–P(6)–Z], for all the molecules are

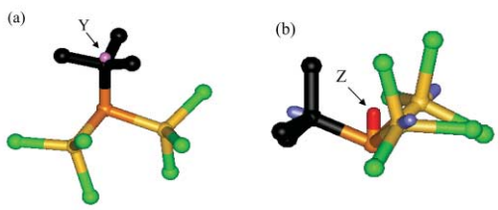

Fig. 5 (a) Point Y lying on the P–C axis at a distance from P equivalent to the P–Si distance and (b) the centroid Z of the Y···Si(7)···Si(8) triangle.

Table 9 Torsions and directional components for tilt angles in $PBu^t(SiH_3)_2$, $PBu^t(SiH_3)(SiCl_3)$ and $PBu^t(SiCl_3)_2$ [a, b, c]

	X, Y = H	X = H, Y = Cl (B)	X = H, Y = Cl (A)	X, Y = Cl
Tilt direction				
V–Si(7)–P(6)–Z	174.9	−151.1	162.6	−133
W–Si(8)–P(6)–Z	−135.4	−142.4	−158.2	−147
X–C(1)–P(6)–Z	−175.2	175.8	158.4	−174
Directional components				
$Si(7)X_3$	4.0, 0.3	4.4, −2.4	3.4, 1.0	4.0, −4.3
$Si(8)Y_3$	3.1, −3.0	4.9, −3.8	4.6, −1.8	4.7, −3.0
$C(1)C_3$	5.6, −0.5	6.2, 0.5	6.2, 2.5	6.6, −0.7

[a] Axial tilt quoted first, followed by equatorial tilt. [b] Positive axial tilt indicates movement towards the lone-pair on phosphorus. Negative equatorial tilt indicates clockwise motion of group as viewed down lone-pair–phosphorus axis. [c] All angles in °.

listed in Table 9, as are the final directional components for all the tilts.

For $PBu^t(SiH_3)_2$, the tilt direction for the *tert*-butyl group is −175°, indicating that the *tert*-butyl group is tilted more or less up towards the lone pair on the phosphorus atom. The $Si(7)H_3$ and $Si(8)H_3$ group torsion angles were 175 and −135°. By resolving these tilts into directional components, information about the effect of steric loading can be gained. For the $Si(7)H_3$ group, there is a 4.0° component towards the phosphorus lone pair, and a 0.3° component around the equatorial belt towards the *tert*-butyl group and away from the $Si(8)H_3$ group. For the $Si(8)H_3$ group, there is an axial component of 3.1°, and an equatorial component of 3.0° away from the *tert*-butyl group and towards the $Si(7)H_3$ group.

For conformer A of $PBu^t(SiH_3)(SiCl_3)$, the tilt direction for the *tert*-butyl group is 158°, and the $Si(7)H_3$ and $Si(8)Cl_3$ group tilt directions are 163 and −158°. These resolve into directional components as follows. The *tert*-butyl group is tilted 6.2° towards the lone pair and 2.5° around the equatorial belt towards the $Si(7)H_3$ group. The $Si(7)H_3$ group is tilted axially 3.4° and equatorially 1.0° away from the *tert*-butyl group and towards the $Si(8)Cl_3$ group. The $Si(8)Cl_3$ group is tilted axially 4.6° and equatorially 1.8° towards the $Si(7)H_3$ group and away from the *tert*-butyl group. For conformer B, the tilt directions are 176, −151 and −142° for the *tert*-butyl, $Si(7)H_3$ and $Si(8)Cl_3$ groups. These lead to directional components of 6.2° and 0.5° for the *tert*-butyl group, indicating that it is tilted mainly towards the lone pair. The $Si(7)H_3$ group is tilted axially 4.4° and equatorially 2.4° towards the *tert*-butyl group and away from the $Si(8)Cl_3$ group. The $Si(8)Cl_3$ group is tilted axially 4.9° and equatorially 3.8° towards the $Si(7)H_3$ group and away from the *tert*-butyl group.

For $PBu^t(SiCl_3)_2$, the tilt direction for the *tert*-butyl group ϕ[X–C(1)–P(6)–Z] is −174°, indicating that the *tert*-butyl group is tilted more or less up towards the lone pair on the phosphorus atom. The $Si(7)Cl_3$ and $Si(8)Cl_3$ groups returned corresponding tilt directions of ϕ[V–Si(7)–P(6)–Z] = −133° and ϕ[W–Si(8)–P(6)–Z] = −147°. For the $Si(7)Cl_3$ group, there is a 3.9° component towards the phosphorus lone pair, and a 4.2° component around the equatorial belt, away from the $Si(8)Cl_3$ group and towards the *tert*-butyl group. For the $Si(8)Cl_3$ group, there is a 4.7° axial tilt and a 3.0° equatorial tilt, the latter being towards the $Si(7)Cl_3$ group and away from the *tert*-butyl group.

In general it can be seen that the tilt of the *tert*-butyl groups, which is the largest of those for the three ligands, is towards the lone pair of the phosphorus, with very little equatorial tilt except in the case of conformer A of $PBu^t(SiH_3)(SiCl_3)$. In this case, the *tert*-butyl group is tilted 2.5° away from the $Si(8)Cl_3$ group and towards the $Si(7)H_3$ group. The $Si(8)Cl_3$ group is also observed to tilt away from the *tert*-butyl group by 1.8°. The combined equatorial tilt is the same for conformer B, with the *tert*-butyl group tilting 0.5° and the $Si(8)Cl_3$ group tilting 3.8°, giving a combined tilt of 4.8° away from each other. The overall distortion in $PBu^t(SiCl_3)_2$ is greater than in $PBu^t(SiH_3)_2$, as would be expected on steric grounds. This distortion manifests itself in an axial direction, with all groups being tilted more towards the phosphorus lone-pair in $PBu^t(SiCl_3)_2$ than in $PBu^t(SiH_3)_2$. Examination of the MP2(fc)/6-311G* energies calculated for all the molecules reveals that disproportionation of $PBu^t(SiH_3)_2$ and $PBu^t(SiCl_3)_2$ to give two molecules of $PBu^t(SiH_3)(SiCl_3)$ is favourable by 13.1 kJ mol^{-1}. This can be attributed again to the fact that $PBu^t(SiCl_3)_2$ has three bulky ligands which destabilises the molecule compared to the product which is less sterically hindered with the silyl group rather than the trichlorosilyl group.

Fig. 1(b) shows a view down the P–C bond of $PBu^t(SiCl_3)_2$, and the butyl group torsion can be seen to bring one of the methyl groups [C(4)] into closer contact with the $Si(7)Cl_3$ group. The equatorial tilt component of this $SiCl_3$ group is towards the *tert*-butyl group, and the equivalent tilt of the $Si(8)Cl_3$ group is away from the *tert*-butyl group. This suggests that it is an attractive force between Cl and H that determines this parameter.

In the related compound $PBu^t_2(SiCl_3)$, the overall tilts are very similar to those in $PBu^t(SiCl_3)_2$.[7] The equatorial components of the tilts in the present example are associated with the $SiCl_3$ groups, whereas in the di-*tert*-butyl case they are associated with the two butyl groups. These groups are tilted away from each other and towards the lone $SiCl_3$ group, which has virtually no equatorial tilt component. The equatorial component therefore can be attributed to mutual repulsion of the two *tert*-butyl groups and to attractive Cl···H interactions.

All the angles at phosphorus in these molecules are generally much smaller than tetrahedral, reflecting the high p-orbital contribution to the bonds. Angles involving the carbon atom of a *tert*-butyl group (C–P–C) are larger than the corresponding C–P–Si, which in turn are larger than Si–P–Si. However, in $PBu^t(SiCl_3)_2$ or $PBu^t_2(SiCl_3)$ the bulky groups are accommodated as much by tilting as by expansion of the angles at phosphorus. The flexibility of these ligands, which allows this tilting, is very important in the accommodation of steric strain in these bulky molecules.

Acknowledgements

We thank Dr V. Typke of the University of Ulm for the variable-array version of ASYM 40.

References

1 B. Beagley, A. G. Robiette and G. M. Sheldrick, *J. Chem. Soc. A*, 1968, 3002.
2 D. W. H. Rankin, A. G. Robiette, G. M. Sheldrick, B. Beagley and T. G. Hewitt, *J. Inorg. Nucl. Chem.*, 1969, **31**, 2351.
3 G. A. Forsyth, H. E. Robertson and D. W. H. Rankin, *J. Mol. Struct.*, 1990, **239**, 209.
4 V. A. Naumov and O. Kataeva, *Zh. Strukt. Khim.*, 1983, **24**(5), 96.
5 H. Oberhammer, R. Schmutzler and O. Stelzer, *Inorg. Chem.*, 1978, **17**(5), 1254.
6 R. Seip, H. Schmidbaur, G. Blaschke, H. E. Robertson and D. W. H. Rankin, *J. Chem. Soc., Dalton Trans.*, 1985, 827.

7 W.-W. du Mont, L. Müller, R. Martens, P. M. Papathomas, B. A. Smart, H. E. Robertson and D. W. H. Rankin, *Eur. J. Inorg. Chem.*, 1999, 1381.
8 R. Martens and W.-W. du Mont, *Chem. Ber.*, 1992, **125**(3), 657.
9 Gaussian 98, Revision A.7, M. J. Frisch, G. W. Trucks, H. B. Schlegel, G. E. Scuseria, M. A. Robb, J. R. Cheeseman, V. G. Zakrzewski, J. A. Montgomery, R. E. Stratmann Jr, J. C. Burant, S. Dapprich, J. M. Millam, A. D. Daniels, K. N. Kudin, M. C. Strain, O. Farkas, J. Tomasi, V. Barone, M. Cossi, R. Cammi, B. Mennucci, C. Pomelli, C. Adamo, S. Clifford, J. Ochterski, G. A. Petersson, P. Y. Ayala, Q. Cui, K. Morokuma, D. K. Malick, A. D. Rabuck, K. Raghavachari, J. B. Foresman, J. Cioslowski, J. V. Ortiz, A. G. Baboul, B. B. Stefanov, G. Liu, A. Liashenko, P. Piskorz, I. Komaromi, R. Gomperts, R. L. Martin, D. J. Fox, T. Keith, M. A. Al-Laham, C. Y. Peng, A. Nanayakkara, C. Gonzalez, M. Challacombe, P. M. W. Gill, B. Johnson, W. Chen, M. W. Wong, J. L. Andres, C. Gonzalez, M. Head-Gordon, E. S. Replogle and J. A. Pople, Gaussian, Inc., Pittsburgh PA, 1998.
10 J. S. Binkley, J. A. Pople and W. J. Hehre, *J. Am. Chem. Soc.*, 1980, **102**, 939.
11 M. S. Gordon, J. S. Binkley, J. A. Pople, W. J. Pietro and W. J. Hehre, *J. Am. Chem. Soc.*, 1982, **104**, 2797.
12 W. J. Pietro, M. M. Francl, W. J. Hehre, D. J. DeFrees, J. A. Pople and J. S. Binkley, *J. Am. Chem. Soc.*, 1982, **104**, 5039.
13 W. J. Hehre, R. Ditchfield and J. A. Pople, *J. Chem. Phys.*, 1972, **56**, 2257.
14 P. C. Hariharan and J. A. Pople, *Theor. Chim. Acta*, 1973, **28**, 213.
15 M. S. Gordon, *Chem. Phys. Lett.*, 1980, **76**, 163.
16 A. D. McLean and G. S. Chandler, *J. Chem. Phys.*, 1980, **72**, 5639.
17 (*a*) NBO Version 3.1, E. D. Glendening, A. E. Reed, J. E. Carpenter and F. Weinhold; (*b*) C. M. Breneman and K. B. Wiberg, *J. Comp. Chem.*, 1990, **11**, 361; (*c*) B. H. Besler, K. M. Merz, Jr. and P. A. Kollman, *J. Comp. Chem.*, 1990, **11**, 431; (*d*) U. C. Singh and P. A. Kollman, *J. Comp. Chem.*, 1987, **8**, 894.
18 C. M. Huntley, G. S. Laurenson and D. W. H. Rankin, *J. Chem. Soc., Dalton Trans.*, 1980, 954.
19 J. R. Lewis, P. T. Brain and D. W. H. Rankin, *Spectrum*, 1997, **15**, 7.
20 S. Cradock, J. Koprowski and D. W. H. Rankin, *J. Mol. Struct.*, 1981, **77**, 113.
21 A. S. F. Boyd, G. S. Laurenson and D. W. H. Rankin, *J. Mol. Struct.*, 1981, **71**, 217.
22 A. W. Ross, M. Fink and R. Hilderbrandt, *International Tables for Crystallography*, ed. A. J. C. Wilson, Kluwer Academic Publishers, Dordrecht, Boston and London, 1992, vol. C, p. 245.
23 (*a*) L. Hedberg and I. M. Mills, ASYM 40, Program for Force Constants and Coordinate Analysis, version 3.0; (*b*) See also L. Hedberg and I. M. Mills, *J. Mol. Spectrosc.*, 1993, **160**, 117.
24 (*a*) N. W. Mitzel, B. A. Smart, A. J. Blake, H. E. Robertson and D. W. H. Rankin, *J. Phys. Chem.*, 1996, **100**, 9339; (*b*) A. J. Blake, P. T. Brain, H. McNab, J. Miller, C. A. Morrison, S. Parsons, D. W. H. Rankin, H. E. Robertson and B. A. Smart, *J. Phys. Chem.*, 1996, **100**, 12280.
25 H. E. Robertson, D. W. H. Rankin, R. Seip, H. Schmidbaur and G. Blaschke, *J. Chem. Soc., Dalton Trans.*, 1985, **4**, 827.
26 Gas-phase Molecular Structures Determined by Electron Diffraction, D. W. H. Rankin and H. E. Robertson, *Spectroscopic Properties of Inorganic and Organometallic Compounds*, 33, ed. G. Davidson, 2000, pp. 500–519.
27 A. R. Campanelli, F. Ramondo, A. Domenicano and I. Hargittai, *Struct. Chem.*, 2000, **11**, 155.
28 M. Dakkouri and R. Bitschenauer, *J. Mol. Struct.*, 2000, **519**, 61.